A Continuous Millimeter-Wave Imaging Scanner for Art Conservation Science

Ayesha Younus, Jean-Pascal Caumes, Simon Salort, Bruno Chassagne, Christophe Pradère, Alain Dautant, Anne Ziéglé, Emmanuel Abraham

Hindawi Publishing Corporation
Advances in Optical Technologies
Volume 2011, Article ID 275682, 9 pages
doi:10.1155/2011/275682

Research Article

A Continuous Millimeter-Wave Imaging Scanner for Art Conservation Science

Ayesha Younus,[1] Jean-Pascal Caumes,[2] Simon Salort,[2] Bruno Chassagne,[2] Christophe Pradère,[3] Alain Dautant,[4] Anne Ziéglé,[5] and Emmanuel Abraham[1]

[1] *Laboratoire Ondes et Matière d'Aquitaine, Université de Bordeaux, CNRS UMR 5798, 351 Cours de la Libération, 33405 Talence, France*
[2] *ALPhANOV, Centre Technologique Optique et Lasers, 351 Cours de la Libération, 33405 Talence, France*
[3] *Laboratoire TRansfert Ecoulements FLuides et Energétique (TREFLE), Université de Bordeaux, CNRS-ENSAM UMR 8508, 33405 Talence, France*
[4] *Institut de Biochimie et Génétique Cellulaires, Université de Bordeaux, CNRS UMR 5095, 1 rue Camille Saint-Saëns, 33077 Bordeaux, France*
[5] *Museum of Aquitaine, 20 Cours Pasteur, 33000 Bordeaux, France*

Correspondence should be addressed to Emmanuel Abraham, em.abraham@loma.u-bordeaux1.fr

Received 31 May 2011; Accepted 27 August 2011

Academic Editor: Krikor Ozanyan

A monochromatic continuous millimeter-wave imaging system coupled with an infrared temperature sensor has been used to investigate artistic objects such as painting artworks or antiquities preserved at the museum of Aquitaine. Especially, 2D and 3D analyses have been performed in order to reveal the internal structure of a nearly 3500-year-old sealed Egyptian jar.

1. Introduction and Background

In the field of art conservation, curators and scientists are forever interested in the material composition and substructure identification for protecting our cultural heritage. This scientific analysis is essential to reveal the history of the object and discover how the artwork has been restored in past centuries. Beyond this, for the restorers, the scientific analysis of the sample composition provides information about the artist's technique and allows an accurate material selection for future restoration.

Various physical methods of diagnosis are frequently used for the purpose of material identification and investigating artists' working methods. Fourier-transform infrared spectroscopy, Raman microscopy [1, 2], and X-ray radiography [3] are some of the commonly used methods for the analysis of artworks. To obtain detailed information about the sample, multiple spectroscopic imaging techniques are generally utilized from X-rays, ultraviolet to infrared [4, 5]. This multispectral imaging method allows us to examine the work of interest under different ranges of electromagnetic wavelengths [6, 7]. Normally all above-mentioned techniques have their own advantages and limitations compared to each others. The suitability of each method can depend on the composition, dimension, condition, and nature of the artifacts under test.

Considering the shortcomings of various methods, terahertz (THz) radiation has emerged as a possible powerful candidate in the field of art conservation for the nondestructive and noninvasive investigation of various art related materials. In art painting, THz radiation can be used to analyze the materials slightly below the layers of the paint, such as preparation layers. It also has the potential for providing depth information from the paint layers. Particularly evident is the scope of the THz technique for the investigation of wall paintings where X-ray radiography cannot be easily applied. THz radiation can provide additional details and complementary spectroscopic data related to each material for a better diagnosis and understanding of an artwork. In cultural heritage science, two main aspects of THz technology can be profitably explored: spectroscopy for the analysis of various artistic materials and noninvasive THz imaging. These

abilities of THz radiation has been demonstrated in variety of research works reported for the analysis of cultural heritage materials [8], such as evaluation of mural paintings [9] or for character recognition in medieval manuscripts [10]. THz radiation is widely applied for the investigation of paintings and spectroscopic analysis of pigments [11, 12]. Recently, Fukunaga and Picollo reported an important THz analysis on the masterpiece *Polittico di Badia* by Giotto exposed at the Uffizi Gallery in Florence [13].

Most of the THz studies related to painting artwork employed a pulsed THz time-of-flight imaging system in order to map the layer by layer substructure of the artwork, find hidden underdrawings, and sometimes spectrally identify pigments, organic/inorganic dyes, and varnish [14, 15]. However, pulsed THz imaging requires a femtosecond laser source associated with a point-by-point scanning procedure to measure a 2D image of the sample. Moreover, the total power of the THz emission is generally limited to nanowatts with pulsed THz systems, which limits the THz detection limit in case of thick or absorbing materials. In this paper, we present a continuous wave (CW) imaging system for the 2D visualization of artistic artworks such as paintings or antiquities. The main advantages of the system are flexibility, strong output power (20 mW), and portable nature so that it can offer essential characteristics for on-site THz imaging of unique artworks. To evaluate the potential of this CW imaging system, we will first present some preliminary results concerning art painting. Then, in collaboration with curators, we will present on-site THz imaging of historical objects performed at the museum of Aquitaine in Bordeaux.

2. Experimental Setup

The experimental setup of the portable millimeter CW imaging system has been described elsewhere [16]. Here, we briefly recall that it is based on a compact millimeter wave Gunn diode (110 GHz, 20 mW) coupled with a horn antenna (Figure 1). The output beam is collimated using an off-axis parabolic mirror M ($f' = 150$ mm) and then focused with a Teflon lens L ($f' = 60$ mm) on the sample S, which is positioned on three-axes XY-θ motorized stages. The angle θ corresponds to a rotation around the vertical Y-axis. At the sample position S, the beam profile is homogeneous with a Gaussian circular shape (4 mm beam diameter, measured at FWHM) in agreement with the theoretical values obtained from the propagation of Gaussian beams. This indicates that the spatial resolution of the millimeter CW scanner is limited to a few millimeters owing to the long wavelength of the emitting source. Consequently, the system is more adapted for the visualization of subcentimeter structures within a larger size object, typically more than (100 mm × 100 mm × 100 mm). Symmetrically, the focal volume is imaged using a similar arrangement on a commercial low-cost pyroelectric sensor (Spectrum Detector Inc.). For final data acquisition, the THz beam is modulated at 20 Hz by an optical chopper, and the amplitude of the transmitted THz is acquired with a lock-in amplifier. A 2D transmission image of the sample is obtained by moving the object in the X and Y directions with a scan step of generally 1 mm in both directions. With a scan speed of 5 pixels/s, the acquisition time for a (100×100) pixels 2D image size is about 30 minutes. This time remains longer than commercial pulsed THz imaging systems since Picometrix proposes a scan speed of 100 pixel/s.

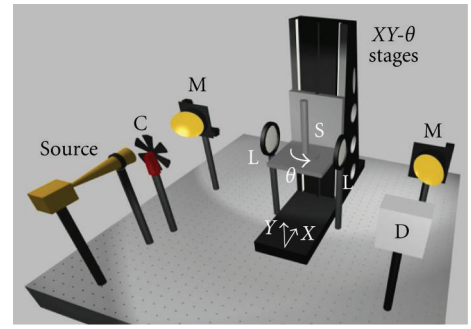

Figure 1: Experimental setup. C: optical chopper, L: Teflon lenses ($f' = 60$ mm), M: off-axis parabolic mirrors ($f' = 150$ mm), S: sample, D: pyroelectric detector coupled to a lock-in amplifier.

For 3D reconstruction, the sample is rotated in order to provide a different visualization of the object. From the tilted series, we are able to construct the sinogram of the object which represents, for a given horizontal slice, the evolution of the transmitted THz amplitude as a function of the rotation angle. Here, to get a reasonable acquisition time for 3D imaging, we selected a rotation step of 10°. In this case, we obtained the corresponding 18 projections in nearly 9 hours. For 3D reconstruction, the back projection of the filtered projections (BFP) has been employed as the standard 3D reconstruction method [17]. This reconstruction process is based on the inverse Radon transform [18], which computes the final pixel values from the filtered projections. It is widely developed in X-Ray CT scan imaging and also commonly used in THz CT since it is available in most CT software tools.

3. Experimental Results

Experimental results are divided into two parts. First, we will present CW imaging of painting artworks using test samples. Then, we will focus on CW imaging of historic objects stored at the museum of Aquitaine.

3.1. CW Imaging of Painting Artworks. In order to illustrate the potential of the CW system for investigating artwork, we first performed THz imaging of test painting samples. For this purpose we used homemade sketches drawn onto canvas and wooden supports. The goal of the study was to demonstrate the potential of the CW imaging system for nondestructive and noninvasive analysis of paintings on canvas and wood supports.

First, we were interested in comparing the CW imaging system with a homemade pulsed THz imaging system based on a femtosecond laser and a time-domain spectrometer [19, 20]. For this purpose, we used another Gunn diode source to pump a frequency tripler in order to deliver 0.2 mW at 240 GHz. The sample consisted in a homemade graphite sketch (woman face) onto a canvas, covered by a patchwork of painting layers with different colours produced with commercially available gouaches (Royal Talens, Van Gogh

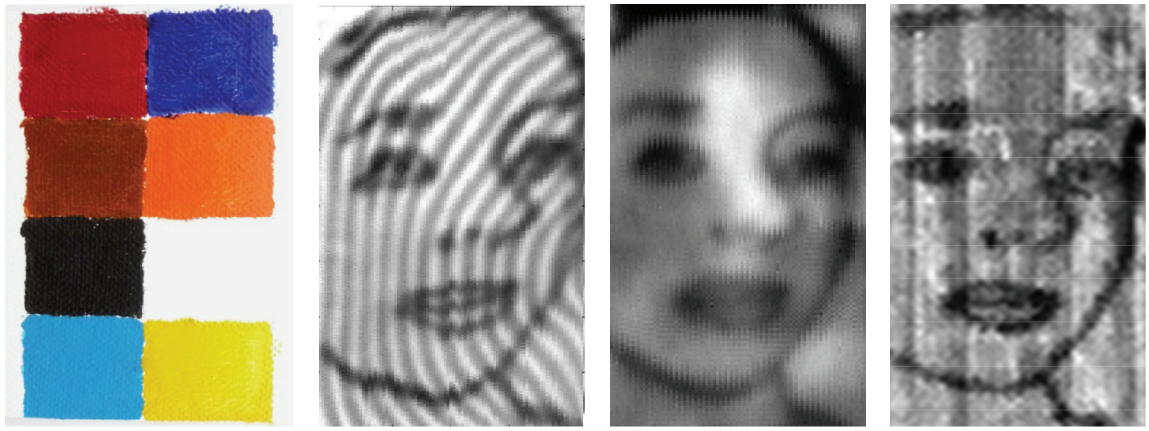

(a) (b) (c) (d)

Figure 2: (a) Photograph of the sample (paint layers covering a graphite sketch), (90 mm × 55 mm); (b) transmission CW image at 240 GHz; (c) transmission CW image after application of a FFT bandpass filter (Image J software) to remove background interference pattern; (d) transmission pulsed THz image at 240 GHz. In (b) to (d), black level indicates a decrease of THz signal.

acrylic colours, Figure 2(a)). Since the actual composition of the painting products is unknown (pigment indexes are reported but no indication on binders), we have to acknowledge that this ignorance might affect the presented results. Figure 2(b) shows the millimeter CW image in transmission mode at 240 GHz. The background interference pattern visible in the image is caused by standing waves in the imaged object and the measurement setup, owing to the long coherence length of the Gunn diode. This interference pattern can be removed by Fourier Transform post-treatment or simply by tilting the sample to avoid these interferences (Figure 2(c)). The fringe pattern also reflects the sample flatness indicating the variations of the local curvature. This could be used for an additional surface analysis of the sample. The graphite sketch is clearly visible for each part of the sample, corresponding to a decrease of the transmitted THz signal. First, it means that the different pigments deposited onto the canvas transmit similarly the incident 240 GHz radiation. Then, it also means that the underlying graphite (6B grade) significantly reflects the 240 GHz radiation due to the high graphite conductivity. For comparison, Figure 2(d) shows the equivalent THz image at 240 GHz obtained with the pulsed THz imaging system. At this frequency, the CW image exhibits a better signal-to-noise ratio compared with the pulsed THz image which presents a poor image quality owing to the low THz signal amplitude at 240 GHz. This illustrates the performance of the CW device, enabling rapid, efficient, and precise inspection of opaque materials.

3.2. Reflection CW Imaging of Canvas Painting. In this section, millimeter CW imaging is performed in reflection mode (30° oblique incidence) at 110 GHz. The sample consists of a painting on canvas whose visible appearance resembles a simple two-colour painting (naphthol red light and oxide black from Royal Talens) (Figure 3(a)). The reflection-based CW image clearly reveals the presence of an underlying sketch (copy of the *Vitruvian* man) produced with a graphite pencil lead (Figure 3(b)). As for the previous transmission experiment, the reflection imaging makes it possible to investigate drawings beneath paintings in order to discover the history of an artwork and discover how it has been technically elaborated. However, in this second experiment, the reflection from the graphite induces an increase of the 110 GHz radiation, whereas in transmission it caused a decrease of the 240 GHz radiation. This explains the inverted grey-level representation of the underlying sketch between Figures 2 and 3.

A finer analysis of Figure 3(b) also reveals the higher reflected signal from the black painting (approximately +10%) compared to the one reflected by the red painting. This indicates that the reflection coefficients of these two commercial paintings are different at 110 GHz. In order to explain the observed variations of the reflection coefficients in relation with the measurement of the painting refractive indexes at 110 GHz, we also measured the reflectance of four different Van Gogh acrylic colours (oxide black, naphthol red, azo yellow light, ultramarine). For this purpose, the colours were used in the form of pellets, filled inside a glass support having some holes inside (Figure 4(a)). Figure 4(b) presents the reflection imaging of the four pellets sample. The white colour indicates an increase of the amplitude of the THz reflected signal. We can visually observe that oxide black has the highest reflectance, then ultramarine as intermediate reflectance, and finally azo yellow light and naphtol red as lowest reflectance. This result is also quantitatively presented in Figure 4(c), which shows the evolution of the measured reflected signal in millivolts.

3.3. CW Imaging of Wooden Panel Painting. The final painting sample is a *Madonna* panel shown in Figure 5(a). The sample has been obtained with the courtesy of Computer Vision and Systems Laboratory (Laval University, Quebec). It consists of a (150 mm × 210 mm × 20 mm) panel made of poplar wood that was coated with the usual priming layers of canvas, gesso and glue traditionally employed in forming paintings. The specimen was originally conceived for the

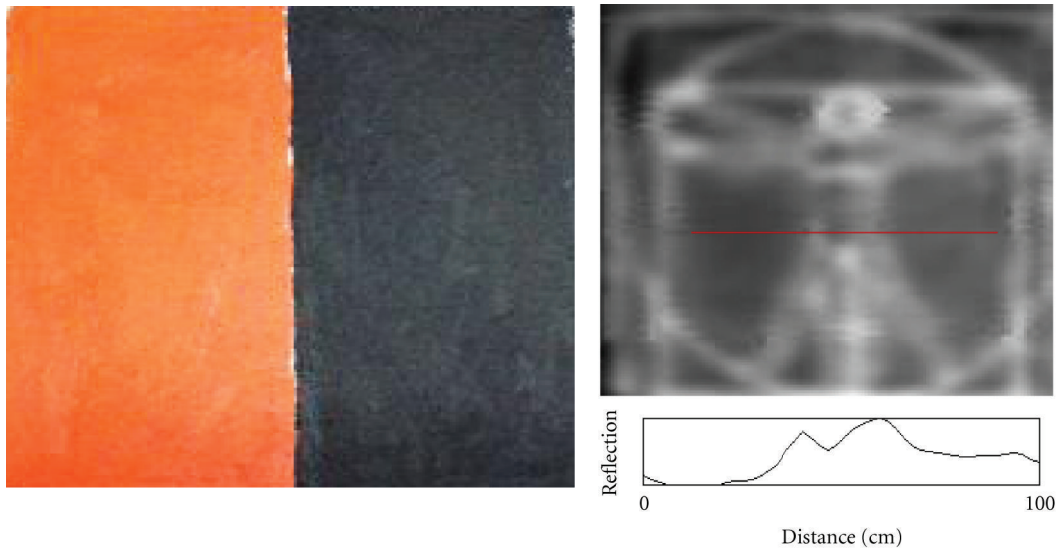

FIGURE 3: (a) Photograph of the sample (paint layers covering a graphite sketch), (150 mm × 150 mm), (b) reflection CW image at 110 GHz revealing the copy of the Vitruvian man. White colour indicates a higher reflection. Variation profile in reflected signal corresponding to the horizontal red line inside the CW image is also shown.

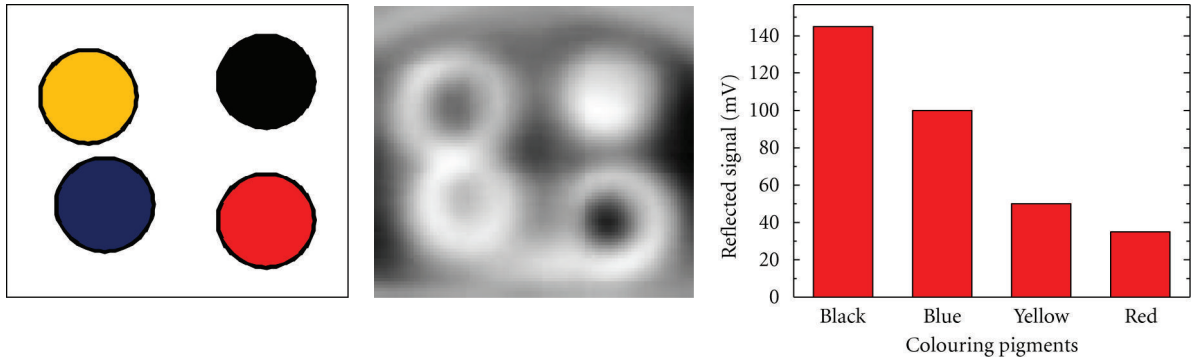

FIGURE 4: (a) Sample design (50 mm × 50 mm), (b) reflection image at 110 GHz, white colour indicating higher reflection, (c) corresponding curve revealing the difference in reflection by various colour pigments.

inspection of subsurface artificially detached regions inside the layered structure simulated by inserting thin Mylar sheets at different depths [21].

Figure 5(b) shows the transmission millimeter CW image of the painting obtained at 110 GHz. We can notice multiple defect areas or flaws in the painting. The corresponding locations of these defects in the photograph are indicated by the red lines. However, from the transmission CW imaging, we can not determine the depth position of these defects. On the right upper corner of the THz image, indicated by the red circle, we can distinguish the headscarf of the Madonna, althought, the contrast is very poor. Figure 5(c) shows the reflection-based CW image of the sample obtained at 110 GHz. In this image, all the previous defects are not visible anymore, indicating that they might be located in depth within the sample. Indeed, in that case the amplitude of the reflected THz beam becomes too low after the round trip travel into the sample. Here, we can distinguish the woman's face and the headscarf and another feature which was not noticed in transmission THz imaging: an additional large defect visible in the right lower corner. However, it is difficult to explain the reason why this defect was not previously revealed in THz transmission imaging (Figure 5(b)).

3.4. CW On-Site Imaging for Inspection of Antiquities. In collaboration with curators, we finally performed on-site imaging at the museum of Aquitaine in Bordeaux (France). There, many historic art samples have been scanned from ancient Egyptian and Roman objects to more contemporary ones. Here, we present a summary of major results obtained at the museum. All the objects have been scanned in a transmission imaging geometry.

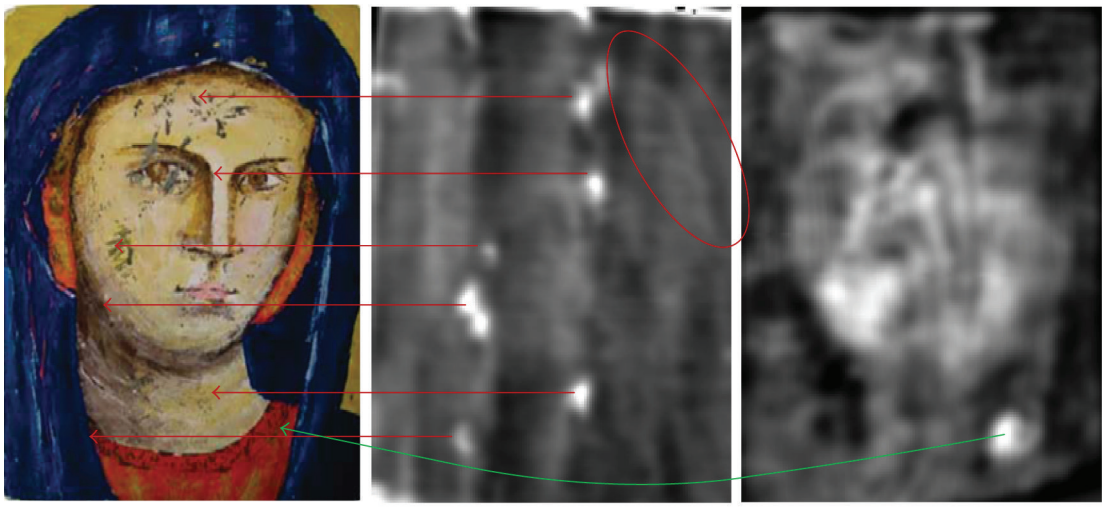

(a) (b) (c)

Figure 5: (a) Photograph of the Madonna painting (courtesy of Laval University, Quebec), (b) transmission CW image obtained at 110 GHz, (c) reflection CW image at 110 GHz (oblique incidence).

(a) (b)

Figure 6: (a) Photograph of the apothecary jar (inventory number 95.34.2), (b) transmission CW image obtained at 110 GHz.

The first sample is a porcelain apothecary jar (museum inventory number 95.34.2, Figure 6(a)). The object, originating from ~1800 AD, is 280 mm in height with a 136 mm diameter. Originally, it was in the drugstore of François Lartigue (1767–1842) in Bordeaux and contained sedative pills of cynoglossum as indicated on the jar. At that time, the roots of this plant were used for their narcotic effects. At present, the jar is closed with a sealed cover and nobody knows its actual contents. Except for the cover, the jar has been fully imaged by the millimeter CW scanner (Figure 6(b)). The THz image reveals an absorbing material occupying the bottom of the jar (white colour in the bottom of Figure 6(b)), which may be attributed to residual cynoglossum pills. However, this content is fixed since the image remains unchanged if the jar is horizontally positioned. We can suppose that after many years in the jar, the pills melt together to form a compact mass at the bottom of the jar. The THz image also reveals the internal shape of the jar with a conical geometry as indicated by the white colour on the left side of the image.

The next samples all come from the Ancient Egyptian collection of the museum. Figure 7(a) presents a photograph of a mummified right hand partly covered by gold leaf and tissues (museum inventory number 96.6.1). The origin of this object, found in the Nile valley in 1898, remains unknown for the curators. However, according to Egyptologists, the presence of the gold leaf at the surface of the hand allows us to suspect that the mummified person was very important, probably belonging to a royal family. The hand size is (202 mm × 78 mm × 29 mm). The THz image reveals the hand skeleton under the dried skin with bones and phalanxes. However, the presence of reflecting gold leaf reduces the transmission of the THz radiation. THz imaging

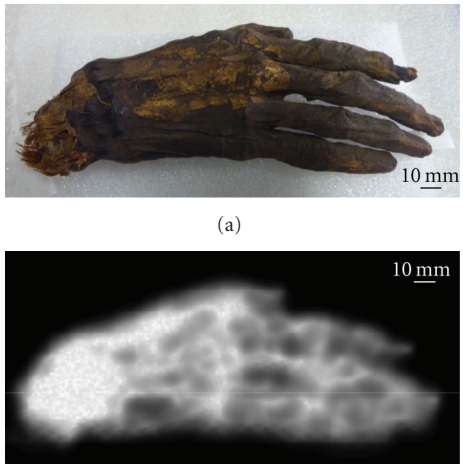

Figure 7: (a) Photograph of the mummified hand (inventory number 96.6.1), (b) transmission CW image obtained at 110 GHz.

of a human mummy hand has been reported in 2010 by Öhrström et al. [22]. The authors already pointed out the poor image quality owing to the thick or optically dense materials.

Figure 8(a) presents a fish sarcophagus in wood (museum inventory number 8599). The object comes from the collection of Dr. Godard (collected in 1861 and bequeathed to the museum of Aquitaine in 1863). The size is (135 mm × 38 mm × 22 mm). The origin of the object remains unknown. The sarcophagus used to contain a mummified fish, but is now empty. The THz image (Figure 8(b)) essentially reveals an absorbing (white colour) material in the central part of the sarcophagus. The corresponding absorbance is plotted in Figure 8(c), defined as $\text{Abs} = \text{Log}_{10}(I_0/I)$, where I_0 is the transmitted signal at 110 GHz measured out of the sample and I is the transmitted signal measured along the red horizontal profile. At the position $x = 90$ mm, the absorbing material exhibits an absorbance of nearly 1.5, attributed to the presence of a wood plug within the sarcophagus. This plug could be originally used to maintain the two pieces of wood constituting the sarcophagus or could have been added in the XIXth century (AD) in order to exhibit the object. In collaboration with Egyptologists, further studies are in progress in order to determine more precisely the origin of this sarcophagus and the practical function of the wood plug revealed by THz imaging.

Finally, we present some results regarding a sealed Egyptian pottery bottle from the XVIIIth Dynasty (New Kingdom period). The original use of this jar remains a mystery for curators. Without any specific decoration, it looks like a simple red-clay vessel hermetically sealed with a clay cork. Its shape (a jar with a neck) indicates that it was most likely used for liquids, not ointment, perfumed cream or unguent because the jar shape would not allow easy access to liquid content for skin application. However, the existence of Menkheperre Tuthmosis III's cartouche (1479–1425 B.C.) on the pottery's clay cork allows us to infer that this object

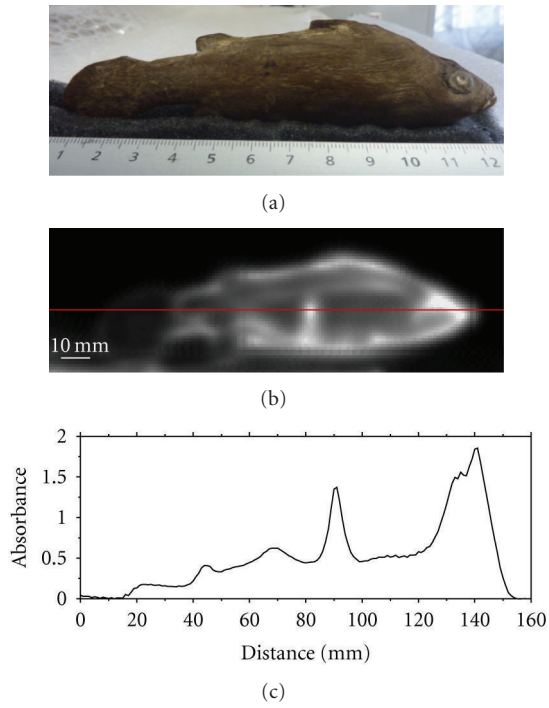

Figure 8: (a) Photograph of the fish sarcophagus (inventory number 8599), (b) transmission CW image obtained at 110 GHz, (c) intensity profile (absorbance) along the horizontal red line.

was very important and may have been used during funerary rites. Indeed, a sticker under the object indicates that it was purchased in 1861 in Gournah, on the famous necropolis of Thebes (on the west bank of Luxor) [23]. Thus, according to experts, this nearly 3500-year-old pottery bottle probably did not contain viscera—usually preserved in specific canopic jars—but most likely food offerings.

The jar (museum inventory number 8608) is presented in Figure 9(a). Its size is 97 mm in height with a maximum diameter of 64 mm. According to curators, shaking of the object indicates that it contains an internal material which is not attached to the pottery. However, X-ray imaging cannot be performed on the sample in order to reveal this internal content, due to irreversible irradiation and consecutive dating alteration. Figures 9(b) and 9(c) present the THz transmission images of the horizontal jar and turned upside-down jar, respectively. These positions have been selected in order to determine the presence of the internal content. As previously explained, due to gravitation effects, a mobile content should move depending on the orientation of the sample. Both images clearly reveal that the jar contains two independent masses, one attached to the bottom and another one free to move inside the internal cavity. Absorbance of both materials can be measured from the horizontal and vertical profiles along the red lines (Figure 9(c)). The fixed bottom material exhibits a global absorbance around 3.4 with a lower absorbance zone (absorbance around 2.3) close to the base of the pot. The origin of the lower density area remains unknown. In the central part of the pottery bottle, the mean absorbance is around 0.8, corresponding to an empty part of

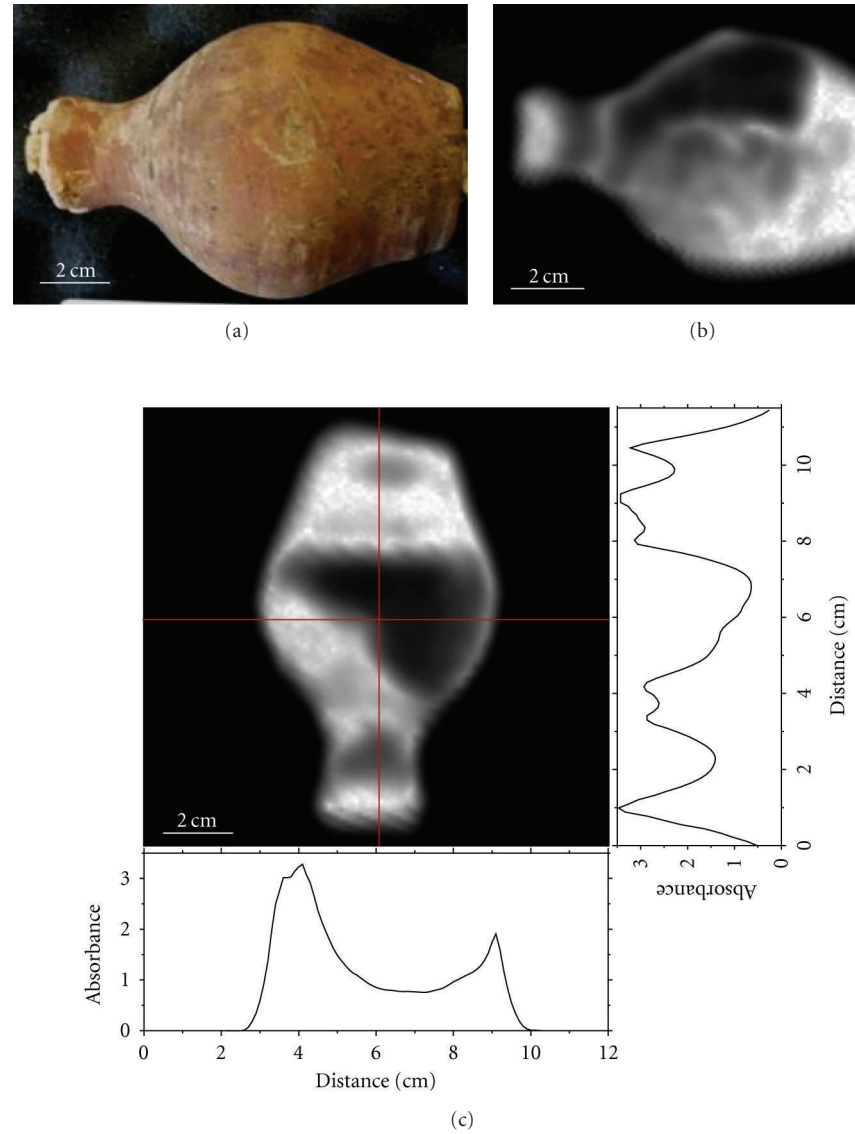

Figure 9: (a) Photograph of the Egyptian jar (inventory number 8608), (b) 2D THz transmission image of the horizontal jar, (c) 2D THz transmission image from the turned upside-down jar and intensity profiles (absorbance) along the horizontal and vertical red lines.

the jar. This absorption is simply attributed to the thickness of the pottery walls. At last, the area concerning the mobile content is characterized by an absorbance around 3.

Here, we would like to emphasize that the THz analysis of the object reveals an important feature concerning the physical aspect of this unidentified mobile content. From Figures 9(b) and 9(c), we can surely affirm that this content is deformable since its shape can fit the inner contour of the pottery bottle. From these absorbance measurements and assuming a constant and homogeneous pottery wall thickness, we can also estimate that the absorbance corresponding to the fixed and mobile contents themselves, without the contribution of the pottery walls, should be around 2.6 and 2.2, respectively.

To evaluate the volume of the internal materials of the second jar, we finally performed a 3D computed tomographic analysis of the object. The tomography has been completed by rotating the object in a turned upside-down position around the vertical axis, in order to reveal the 3D geometrical aspects of both solid and mobile contents, previously identified using 2D THz imaging. From these projection data, we were able to reconstruct and visualize the volume of the jar. Figure 10(a) represents the 3D THz image of the complete object obtained with a volume rendering software. From the reconstruction, the internal volume of the bottle has been estimated to 650 cm^3. With the volume rendering software, it is also possible to visualize independently the different parts of the object. Figure 10(b) presents the 3D THz image of the bottom solid content of the

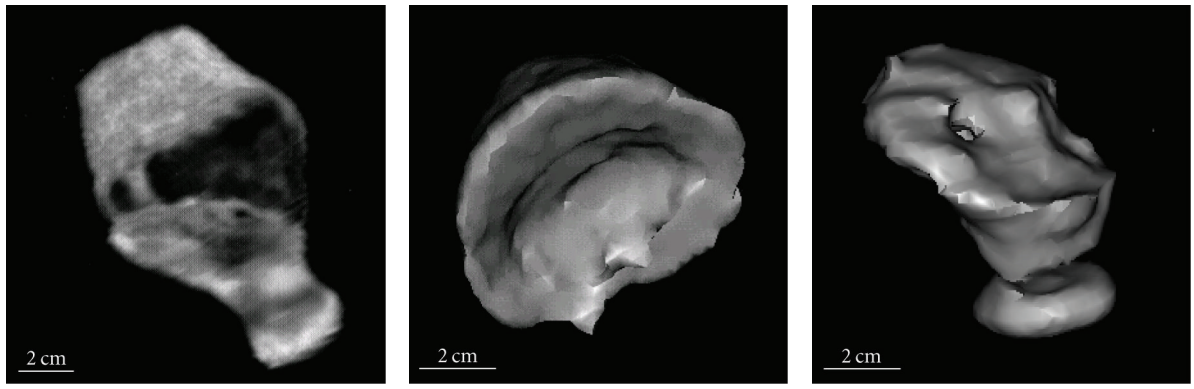

(a) (b) (c)

Figure 10: 3D THz computed tomography of the Egyptian jar (inventory number 8608), turned upside down. (a) Complete 3D reconstruction of the jar. (b) 3D reconstruction of bottom jar content. (c) 3D reconstruction of mobile content.

jar with an estimated volume of 125 cm^3. Moreover, the 3D reconstruction makes it possible to reveal a trough in the central part of this content, which was not visible from the 2D THz images in Figure 9. Finally, Figure 10(c) presents the 3D THz image of the deformable mobile content with an estimated volume of 25 cm^3. As explained previously, from the tilted series and the 3D reconstructions, we can now measure the dimensions of the fixed and mobile contents of the jar and the global thickness of the pottery wall. Assuming that the thickness of the pottery wall varies from 5 to 8 mm, we first can estimate the 110 GHz absorption coefficient α of the jar wall according to the expression $\text{Abs} = \alpha \cdot l$ where l is the distance the THz wave travels through the materials. For the pottery wall, taking into account measurement uncertainties, we found $\alpha = 1.3 \pm 0.3\,\text{cm}^{-1}$, the large uncertainty coming from the difficult evaluation of the wall thickness owing to the limited transverse spatial resolution. Taking into account this wall absorbance, we can finally deduce the 110 GHz absorption coefficients of the internal contents. For the fixed and the mobile contents, taking into account measurement uncertainties, we found the same absorption coefficient $\alpha = 0.70 \pm 0.15\,\text{cm}^{-1}$. This result indicates that the fixed and mobile contents could be constituted by the same material, even if its nature remains unknown. As previously explained, according to Egyptologists, these contents could consist of residual dried materials, probably organic, resulting from possible funerary offering. At present, to further investigate the pottery's origin, the irreversible opening of the jars should be necessary in order to perform complementary chemical analysis of the internal contents.

4. Conclusion

We presented the ability of a compact millimeter CW imaging system for nondestructive and noninvasive analysis of objects related to art conservation. In art painting, hidden underdrawings and sketches can be revealed beneath multiple layers of paintings. The system has also demonstrated its potential for on-site imaging of historical objects stored at the museum of Aquitaine. Especially, the measurements revealed the internal content of a 3500-year-old Egyptian sealed jar. This emphasizes the major role of THz radiation for applications in anthropology and paleontology where the X-ray gold standard is not recommended owing to the fragility/uniqueness of the objects and the problem of sample radiometric dating after X-ray irradiation.

Acknowledgments

The authors gratefully acknowledge François Hubert, Director of the museum of Aquitaine, and the city of Bordeaux for the authorization to perform the measurements at the museum. They also acknowledge Magalie Rouillon and Theo Goltzman for additional fruitful discussions concerning the description of the Egyptian jar and Patrick Mounaix for the loan of the 240 GHz source. This work was supported by the Action Interdisciplinaire de Recherche Archéométrie (TeraScan project, CNRS, France).

References

[1] R. J. H. Clark, "The scientific investigation of artwork and archaeological artefacts: Raman microscopy as a structural, analytical and forensic tool," *Applied Physics A*, vol. 89, no. 4, pp. 833–840, 2007.

[2] L. Burgio, K. Melessanaki, M. Doulgeridis, R. J. H. Clark, and D. Anglos, "Pigment identification in paintings employing laser induced breakdown spectroscopy and Raman microscopy," *Spectrochimica Acta. Part B*, vol. 56, no. 6, pp. 905–913, 2001.

[3] M. P. Morigi, F. Casali, M. Bettuzzi, R. Brancaccio, and V. D'Errico, "Application of X-ray Computed Tomography to Cultural Heritage diagnostics," *Applied Physics A*, vol. 100, no. 3, pp. 653–661, 2010.

[4] A. Pelagotti, L. Pezzati, A. Piva, and A. Del Mastio, "Multispectral UV fluorescence analysis of painted surfaces," in *Proceedings of 14th European Signal Processing Conference (EUSIPCO '06)*, Florence, Italy, September 2006.

[5] J. K. Delaney, J. G. Zeibel, M. Thoury et al., "Visible and infrared imaging spectroscopy of picasso's harlequin musician: mapping and identification of artist materials in situ," *Applied Spectroscopy*, vol. 64, no. 6, pp. 584–594, 2010.

[6] C. Fischer and I. Kakoulli, "Multispectral and hyperspectral imaging technologies in conservation: current research and potential applications," *Reviews in Conservation*, vol. 7, pp. 3–16, 2006.

[7] A. Pelagotti, A. D. Mastio, A. De Rosa, and A. Piva, "Multispectral imaging of paintings: a way to material identification," *IEEE Signal Processing Magazine*, vol. 25, no. 4, pp. 27–36, 2008.

[8] J. M. Manceau, A. Nevin, C. Fotakis, and S. Tzortzakis, "Terahertz time domain spectroscopy for the analysis of cultural heritage related materials," *Applied Physics B*, vol. 90, no. 3-4, pp. 365–368, 2008.

[9] J. B. Jackson, M. Mourou, J. F. Whitaker et al., "Terahertz imaging for non-destructive evaluation of mural paintings," *Optics Communications*, vol. 281, no. 4, pp. 527–532, 2008.

[10] K. Fukunaga, Y. Ogawa, S. Hayashi, and I. Hosako, "Application of terahertz spectroscopy for character recognition in a medieval manuscript," *IEICE Electronics Express*, vol. 5, no. 7, pp. 223–228, 2008.

[11] K. Fukunaga, Y. Ogawa, S. Hayashi, and I. Hosako, "Terahertz spectroscopy for art conservation," *IEICE Electronics Express*, vol. 4, no. 8, pp. 258–263, 2007.

[12] W. Köhler, M. Panzer, U. Klotzach et al., "Non-destructive investigation of paintings with THz-radiation," in *Proceedings of the European Conference on Nondestructive Testing*, p. 181, 2006.

[13] K. Fukunaga and M. Picollo, "Terahertz spectroscopy applied to the analysis of artists' materials," *Applied Physics A*, vol. 100, no. 3, pp. 591–597, 2010.

[14] A. J. L. Adam, P. C. M. Planken, S. Meloni, and J. Dik, "TeraHertz imaging of hidden paint layers on canvas," *Optics Express*, vol. 17, no. 5, pp. 3407–3416, 2009.

[15] J. Labaune, J. B. Jackson, S. Pagès-Camagna, I. N. Duling, M. Menu, and G. A. Mourou, "Papyrus imaging with terahertz time domain spectroscopy," *Applied Physics A*, vol. 100, no. 3, pp. 607–612, 2010.

[16] A. Younus, S. Salort, B. Recur et al., "3D millimeter wave tomographic scanner for large size opaque object inspection with different refractive index contrasts," in *Millimetre Wave and Terahertz Sensors and Technology III*, K. A. Krapels and N. A. Salmon, Eds., vol. 7837 of *Proceeding of SPIE*, 2010.

[17] G. T. Herman, *Image Reconstruction from Projections: The Fundamentals of Computerized Tomography*, Academic Press, 1980.

[18] J. Radon, "Über die Bestimmung von Funktionen durch ihre Integralwerte langs gewisser Mannigfaltigkeiten," *Berichte über die Verhandlungen der Sächsische Akademie der Wissenschaften*, no. 69, pp. 262–277, 1917.

[19] E. Abraham, A. Younus, A. El Fatimy, J. C. Delagnes, E. Nguéma, and P. Mounaix, "Broadband terahertz imaging of documents written with lead pencils," *Optics Communications*, vol. 282, no. 15, pp. 3104–3107, 2009.

[20] E. Abraham, A. Younus, J. C. Delagnes, and P. Mounaix, "Non-invasive investigation of art paintings by terahertz imaging," *Applied Physics A*, vol. 100, no. 3, pp. 585–590, 2010.

[21] A. Ebeid, S. Rott, E. Talmy, C. Ibarra-Castanedo, A. Bendada, and X. Maldague, "Near infrared imaging for multi-polar civilian applications," in *the 10th International Conference on Quantitative Infrared Thermography*, July 2010.

[22] L. Öhrström, A. Bitzer, M. Walther, and F. J. Rühli, "Technical note: terahertz imaging of ancient mummies and bone," *American Journal of Physical Anthropology*, vol. 142, no. 3, pp. 497–500, 2010.

[23] F. Saragoza, "La collection thébaine du Dr Godard au musée d'Aquitaine," *Revue Archéologique de Bordeaux, tome IC*, pp. 131–151, 2008 (French).